EVALUATION OF A METHOD TO EXTRACT PERFORMANCE DATA FROM DYNAMIC MANEUVERS FOR A JET TRANSPORT AIRCRAFT

Ir. J.H. Breeman and Dr.Ir. J.L. Simons
National Aerospace Laboratory
Amsterdam, the Netherlands

Abstract of paper

A very accurate measurement system and a data reduction method have been developed to extract performance data from a single dynamic maneuver, in order to reduce the large amount of flight hours required for the determination of these data by means of measurements in steady flight. In order to evaluate the applicability of this method to a modern jet transport aircraft, a test program has been carried out with the prototype of the Fokker F28 Fellowship. Preliminary results, based on lift-drag polars, show an excellent agreement between the new developed method and "traditional" measurements in steady flight.

0. Introduction

The determination of the performance of an aircraft from dynamic maneuvers has been under development since 1950[1]. The first investigations by the National Aerospace Laboratory (NLR) date from 1957[2]. In later years the Delft University of Technology has developed a method for determining the aircraft performance from dynamic maneuvers.

The essence of this method is the separation of the flight path reconstruction and the estimation of the aerodynamic characteristics of the aircraft. This method has been applied to small and relatively rigid aircraft like the De Havilland DHC-2 Beaver and the Hawker Hunter.[3][4][5]

FIG. 1 FOKKER F 28 FELLOWSHIP

Straightforward determination of aircraft performance from the aerodynamic model has limited accuracy due to nonsteady and nonlinear aerodynamic effects, and measurement errors. However reduction of "quasi steady" dynamic flight conditions to steady-state flight conditions with the aid of the aerodynamic model and the use of more accurate measurement equipment remove the two mentioned drawbacks and opens the way towards performance determination from a small number of dynamic maneuvers, thus reducing the required number of flight hours.

In order to evaluate the applicability of this method to a modern two-engined jet transport aircraft, a short test program was flown in the A1 prototype of the Fokker F28 Fellowship. (Fig 1). In this test program measurements were performed in steady-state and in dynamic flight conditions. This paper discusses the following aspects:

(i) Instrumentation system

As pointed out above and in the literature a necessary condition for accurate performance determination is accurate measurement of quantities like acceleration, angular rates, altitude variation, air speed and engine thrust. Therefore, a special instrumentation system has been developed at NLR which will be briefly discussed in section 1.

(ii) Flight test technique

The developed maneuvers are a compromise between two requirements. Firstly they must be dynamic of nature such that they cover a particular part of the aerodynamic model. Secondly they must be "quasi-steady", that is, close to steady-state flight conditions in order to minimize the influence of large deviations from these conditions. Section 2 will discuss the selection of these flight maneuvers in detail.

(iii) Flight path reconstruction

After transformation of transducer output signals of the data acquisition system into equivalent physical quantities, the flight path can be reconstructed. Application of the square-root information formulation of the fixed interval kalman filter/smoother yields accurate time histories of quantities like the angle of attack and the angle of pitch, which can not be directly measured in flight with the desired accuracy. This flight path reconstruction is discussed in section 3.

(iv) Aerodynamic model identification and calculation of aircraft performance characteristics

The identification of the aerodynamic model starts with the assumption that a relatively simple function of the state variables provides an accurate prediction of the aerodynamic coefficients. The actual coefficients in the chosen polynomial function have been determined with the aid of least squares approximation. The whole identification proces is interactive and adaptive and as such a flexible combination of human intelligence and calculation speed of modern computers. This identification process and the subsequent straightforward reduction to steady-state flight conditions and calculation of lift and drag coefficients is the subject of section 4

(v) Preliminary results of comparison with measurements in steady flight

In this section a lift-drag polar is presented

from data in dynamic flight and from data in steady flight. A comparison of numerical values and accuracy will be given.

The study, as described in this paper, shows that the combination of accurate instrumentation techniques, modern estimation and control theory and advanced mathematical methods is capable of accurate determination of the performance of a jet transport aircraft in a number of flight hours, relatively small in comparison with traditional methods.

1. Instrumentation System

1.0 Introduction. The prototype of the Fokker F28 Fellowship, the F28-A1, is equipped with an ageing instrumentation system, used in all certification and evaluation tests during the development program. This system was not suited for the registration of dynamic measurements, because of the low sampling rates, the inaccurate inertial sensors and air data systems and the ageing control surface transducers. As a consequence, as far as performance and stability and control parameters are concerned, a very accurate instrumentation system was developed in the time span of one year. (See Fig 2)

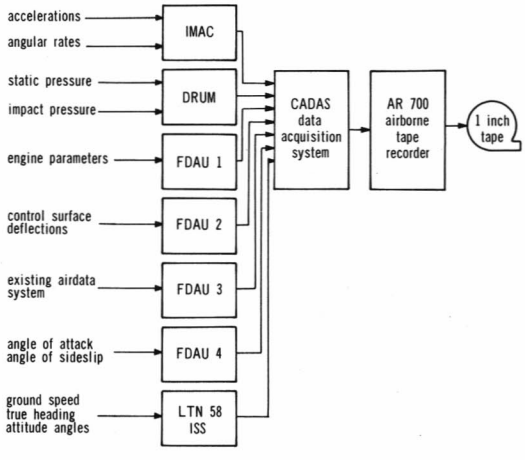

FIG. 2 INSTRUMENTATION SYSTEM

Completely new developments for the project were the Inertial Measurement and Conditioning System (IMAC) and the Air Data Measurement System (DRUM). The other measurement variables, such as the engine parameters and the control surface deflections, were measured by the existing system consisting of 4 Flight Data Acquisition Units (FDAU), which were modified for improved accuracy and sampling rates. Finally a Litton LTN-58 Inertial Sensor System (ISS) was included in order to evaluate the possibility of using a standard inertial navigation system for the measurement of performance and stability and control parameters. The instrumentation was built around the Computer-controlled Avionics Data Acquisition System (CADAS), which was developed by NLR for an earlier project[6]. A complete list of measured variables is given in table 1.

1.1 Inertial Measurement and Conditioning System. The Inertial Measurement and Conditioning System (IMAC) includes three main units, the Inertial Measuring Unit (Dutch acronym IME), the associated control electronics and the signal conditioning and digitizer unit[7].

The IME (see Fig 3) consists of three linear accelerometers (SAGEM 10625 A) measuring Ax, Ay and Az and three rate gyroscopes (Honeywell DGG87B7 wide angle miniature rate integrating gyros) measuring p, q and r mounted on a dural block, which is regulated to a temperature of 74 $\pm$ 0,3°C. The gyroscopes themselves are stabilized to a temperature of 82 $\pm$ 0,3°C. The alignment of the sensors axis with respect to the mounting base is accurate to within 0,002 degree. The IME can be aligned with respect to the aircraft's body reference axis to within 0,01 degree with the aid of adjustable attachments. The IME was mounted in close proximity to the aircraft's center of gravity in order to eliminate as much as possible the effect of elastic deformation of the aircraft on the measurements.

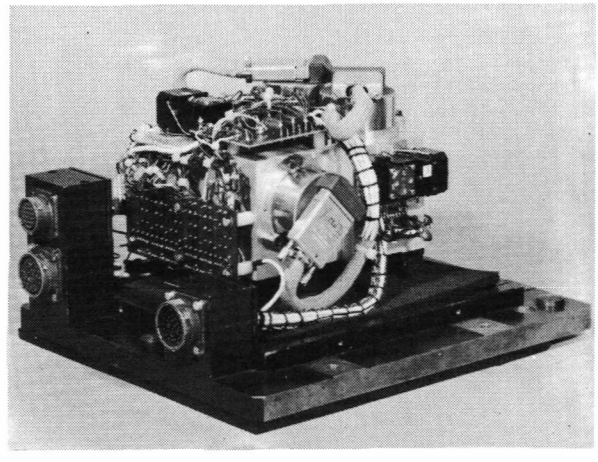

FIG. 3 INERTIAL MEASURING UNIT

The associated control electronics unit contains the gyro and accelerometer feedback electronics, gyro spin motor power supply and the temperature control circuits.

The signal conditioning and digitizer unit contains highly accurate 4 pole analog filters with a cut-off frequency of 15 Hz for each of the 6 sensor channels, which achieve a 92 dB rejection of the sampling frequency of 64 Hz, as well as an equalization of the group delay of the gyro and accelerometer channels to within 1 ms. The stability of gain and offset of the analog filters is within 3.10^{-5} of full scale over the range of operating conditions.

After filtering, the six channels are sampled at a rate of 64 samples per second, with a 16 bit analog to digital convertor. This results in a resolution of 3.10^{-4} deg s^{-1} for the rate gyros and a resolution of 8.10^{-4} m s^{-2} for the accelerometers. Finally the measurement data, along with the status information is transmitted to the CADAS system over

a serial data bus conforming to the ARINC 419 standard.

A series of six calibrations of the complete IMAC system before, during and after the test flights confirmed that the specified static accuracies of 10^{-3} deg s^{-1} for the rate gyros and 10^{-3} ms^{-2} for the accelerometers were achieved.

TABLE 1 LIST OF MEASURED VARIABLES

No.	Measured variable	Computer ident.	Data acquisition	Transducer	Unit	Range	Sample freq.	Static accuracy
11	PRESS.ALT.COARSE	PAC	FDAU 2	KOLLSMAN	m	0-24.000	1	5
12	PRESS.ALT.FINE	PAF	FDAU 2	KOLLSMAN	m	0-600	8	
13	IND.AIRSP.COARSE	IASC	FDAU 2	KOLLSMAN	ms^{-1}	0-230	1	0.5
14	IND.AIRSP.FINE	IASF	FDAU 2	KOLLSMAN	ms^{-1}	31	4	
15	TOTAL AIR TEMP.	TAT	FDAU 2	ROSEMOUNT	K	190-330	1	0.3
16	HEADING	HDG	FDAU 1	COMPASS (FO)	deg	±180	1	1
17	ANGLE OF ROLL	AR	FDAU 2	A 14 GYRO	deg	±45	1	0.5
18	ANGLE OF PITCH	AP	FDAU 1	A 14 GYRO	deg	±45	1	0.5
19	RATE OF ROLL	RR	IMAC	HONEYWELL	deg s^{-1}	±10	64	0.001
20	RATE OF PITCH	RP	IAMC	HONEYWELL	deg s^{-1}	±10	64	0.001
21	RATE OF YAW	RYA	IMAC	HONEYWELL	deg s^{-1}	±10	64	0.001
22	ANGLE OF ATTACK	AA	FDAU 1	SYNCHRO	deg	-5/+25	16	0.03
23	ANGLE OF SIDE SLIP	AS	FDAU 1	SYNCHRO	deg	±15	8	0.03
24	ACCEL.IN X-AXIS	AX	IMAC	SAGEM	ms^{-2}	±25	64	0.001
25	ACCEL.IN Y-AXIS	AY	IMAC	SAGEM	ms^{-2}	±25	64	0.001
26	ACCEL.IN Z-AXIS	AZ	IMAC	SAGEM	ms^{-2}	±25	64	0.001
27	LEFT ENG.SP.LP SHAFT	NLP1	FDAU 1	TACHO	rpm	1600-890	2	9
28	RIGHT ENG.SP.LP SHAFT	NLP2	FDAU 2	TACHO	rpm	1600-890	2	9
29	LEFT ENG.SP.HP SHAFT	NHP1	FDAU 3	TACHO	rpm	2300-1300	1	13
30	RIGHT ENG.SP.HP SHAFT	NHP2	FDAU 3	TACHO	rpm	2300-1300	1	13
31	TURBINE GASTEMP.L.	TGT1	FDAU 3	THERMOCOUPLE	K	573-1023	1	5
32	TURBINE GASTEMP.R.	TGT2	FDAU 3	THERMOCOUPLE	K	573-1023	1	5
33	THRUST PRESS.L.	P7-1	FDAU 3	GULTON	kPa	0-240	8	0.2
34	THRUST PRESS.R.	P7-2	FDAU 3	GULTON	kPa	0-240	8	0.2
35	DELIV.PRESS.LP.COMP.L.	P2-1	FDAU 3	BEAUDOUIN	kPa	0-175	8	2
36	DELIV.PRESS.LP.COMP.R.	P2-2	FDAU 3	BEAUDOUIN	kPa	0-175	8	2
37	DELIV.PRESS.HP.COMP.L.	P3-1	FDAU 3	BEAUDOUIN	kPa	0-1600	8	20
38	DELIV.PRESS.HP.COMP.R.	P3-2	FDAU 3	BEAUDOUIN	kPa	0-1600	8	20
39	STABILIZER DEFL.	DS	FDAU 2	SYNCHRO	deg	-10/+4	4	0.05
40	ELEVATOR DEFL.RIGHT	DE2	FDAU 2	SYNCHRO	deg	-26/+14	16	0.1
41	AILERON DEFL.LEFT	DA1	FDAU 1	SYNCHRO	deg	-22/+22	4	0.3
42	AILERON DEFL.RIGHT	DA2	FDAU 1	SYNCHRO	deg	-22/+22	4	0.3
43	RUDDER DEFL.	DR	FDAU 2	SYNCHRO	deg	-33/+33	4	0.2
44	IMPACT PRESSURE	PI	DRUM	DRUCK	kPa	0-18	16	0.010
45	DEVIATION FROM PS	DPS	DRUM	DRUCK	kPa	±5	16	0.001
46	STATIC PRESSURE	PS	DRUM	ROSEMOUNT	kPa	15-110	16	0.050
47	ELEVATOR DEFL.LEFT	DE 1	FDAU 1	SYNCHRO	deg	-26/+14	16	0.1
48	ANGLE OF PITCH 1	AP11S	FDAU 4	LTN 58	deg	±90	1	1.0
49	ANGLE OF PITCH 4	AP41S	FDAU 4	LTN 58	deg	±25	1	0.1
50	ANGLE OF ROLL 1	AR11S	FDAU 4	LTN 58	deg	±90	1	1.0
51	ANGLE OF ROLL 4	AR41S	FDAU 4	LTN 58	deg	±25	1	0.1
52	N-S. VELOCITY	VNS	ISS	LTN 58	ms^{-1}	0-1600	6	1
53	E-W. VELOCITY	VEW	ISS	LTN 58	ms^{-1}	0-1600	6	1
54	TRUE HEADING	HDGT	ISS	LTN 58	deg	±180	6	0.2
55	PRESENT POS.LAT.	LAT	ISS	LTN 58	deg	±90	6	0.02
56	PRESENT POS.LONG.	LON	ISS	LTN 58	deg	±180	6	0.02

1.2 Air Data Measurement System. The Air Data Measurement System (Dutch acronym "DRUM", see Fig 4) is a full size ATR box which contains pressure sensors, associated electronics and signal conditioning in a temperature controlled environment.

Because of the importance of altitude variations for the flight path reconstruction, a pressure reference vessel is included in DRUM. This vessel is connected to the static pressure until the beginning of a measurement, when it is closed by means of a scannivalve pressure switch. A differential pressure transducer (Druck PPCR 22) with a range of ± 5 kPa measures the difference DPS of the static pressure and the pressure reference. The temperature of the pressure reference vessel is actively regulated to within 0,001 K in order to achieve the desired stability

of 1 Pa, consistent with the transducer accuracy. The measurement of DPS is used to calculate the pressure altitude variation Δha.

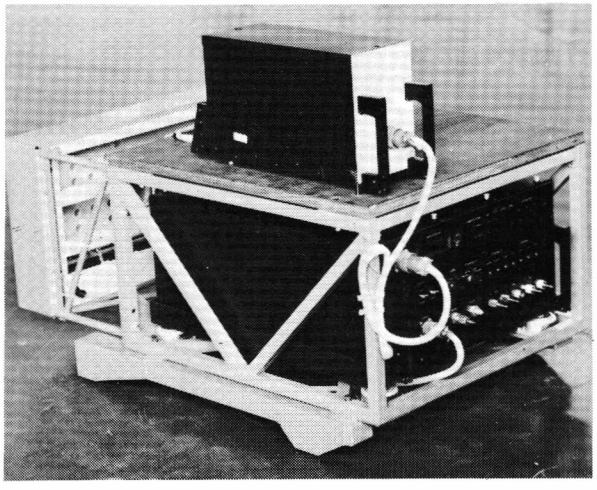

FIG. 4 AIR DATA MEASUREMENT SYSTEM

The absolute static pressure (PS) transducer is a Rosemount 1201 F, which promised a differential accuracy approaching that of the differential pressure system together with a 103 kPa full scale range. Due to transients in the sensor output during accelerations however, the achieved accuracy was in the order of 50 Pa.

The impact pressure (PI) is measured by a DRUCK PDCR 22 transducer with a full scale range of 17 kPa. This sensor showed a marked turn-on behaviour lasting about an hour after which an accuracy in the order of 10 Pa was achieved. The measurement of PI is used to calculate the airspeed Va.

In order to correct for the zero offset of the PI and DPS transducers a special nulling is performed before and after each measurement.

The pressure inputs of these transducers are short circuited by means of a scannivalve pressure switch under full control of the CADAS system, obviating the need for any operator action.

The sensor output signals are filtered by 5 pole Bessel filters with a cut-off frequency of 4 Hz. The group delay of the filters are equal to within 1 ms and the stability of gain and offset are 3.10^{-5} of full scale over the range of operating conditions. The filtered signals are sampled by a 16 bit analog to digital convertor with a sampling rate of 16 Hz. The digitized data along with status and vessel temperature is then transmitted to CADAS over a serial data bus conforming to ARINC 419.

A special feature of DRUM is that the control of the A/D convertor, the scannivalve pressure switch and the data formatting and transmission is performed by a 6800 8 bit microprocessor. Since this processor is only moderately busy with these tasks, it offers a possibility for future expansion, e.g. built-in transducer calibration and zero correction and air data computation.

The static pressure is sensed by a trailing cone which is attached to the top of the vertical fin. Two flights, dedicated to the determination of the Position Error Correction, revealed that the correction was negligeable for this arrangement. The impact pressure is sensed by a direction insensitive pitot tube mounted on the nose of the aircraft.
Since the static system had a total length of 42 m, it was decided to equalize the time delays by using an equal length of tubing for the pitot system. After the flight test program the transfer function of the pitot-static system was measured on the ground, which showed that the time delay varied from 0,6 to nearly 2 seconds as a function of altitude.

1.3 Other Measured Variables. The existing instrumentation system was extensively modified for this project. The 4 Flight Data Acquisition Units (FDAU) were improved in accuracy and sampling rates.

Although the engine parameters are of vital importance for the measurement of performance, it was not possible to change the Rolls Royce installed sensors in the engines. However, the engine thrust calibration was verified on the ground prior to the flight test program.

In order to compare direct measurements with the calculated angle of attack, angle of attack and angle of sideslip vanes were mounted on the nose boom of the F-28. The improved synchro pick-offs proved to be accurate to within $0,03^{o}$.

Accurate measurements of the control surface deflections are needed to enable the aerodynamic model identification. However, the transducers of the control surface deflections of the F-28 were nearly worn out. Therefore, the synchros, gear trains and all mechanical linkages were renewed. Calibration results show that accuracies of $0,05^{o}$ were achieved for some variables.

An Inertial Sensor System (ISS) can be used for the measurement of performance and stability and control parameters. In order to evaluate this possibility a Litton LTN58 ISS was included in the system. The outputs of the ISS are ground speed components, vertical acceleration, true heading, angle of pitch and angle of roll. The actual evaluation has not yet been performed.

1.4 CADAS. The Computer-controlled Avionics Data Acquisition System (CADAS)[6] was used in the instrumentation system. This system consists of a ROLM 1601 airborne computer with its associated interfaces, an Ampex AR-700 1 inch tape recorder and a control/display panel. An important feature of this system is its modularity, since all sensor data is acquired via standardized interfaces (e.g. ARINC 419).

All data from the sensor systems is read by the computer under interrupt control. The computer then adds identification labels and time information to the data before recording it on magnetic tape. The computer is in complete control of the modes of the instrumentation system, as well as of the tape recorder. This was used for the automatic nulling sequence before and after each measurement. The data from all sensor systems can be displayed

at the control/display panel in a standardized format.

2. Flight Test Technique

2.0 Introduction. In the dynamic flight test maneuver, as developed by Delft University of Technology, the aircraft is slowly accelerated from nearly steady flight at low speed approximately 10 % above the stalling speed of the aircraft (1,1 V_S) to the maximum allowable or practical airspeed. At a number of different airspeeds the aircraft is excited in pitch by suitably chosen elevator deflections. In the intervals between the pitch excitations the aircraft's motion is quasi-steady and, therefore, these intervals are suitable for the determination of performance data. The pitch excitations are used to determine the stability and control characteristics.

Earlier experience with dynamic maneuvers with the Hawker Hunter indicated that the combination of an accelerated run with pitch excitation sometimes is detrimental to the precision with which these maneuvers are performed. This would be true especially for the larger F28, as was confirmed in preliminary discussions with Fokker pilots.

Furthermore, performing pitch excursions at low speed with one engine inoperative could lead to a dangerous flight condition. Therefore, it was decided to separate the two parts of the maneuver into separate measurements performed with only a small delay in between.

2.1 Accelerated Run. During an accelerated run the complete speed range of the aircraft for a single configuration is covered. In the design of the test procedure for an accelerated run the following constraints had to be taken into account:

- Stabilization of the engines: Turbofan engines require several seconds to accelerate from the low power setting corresponding to steady flight at low speed to the desired high power setting. Additional time is required for a complete stabilization of all engine parameters.
- Range of DPS transducer: As noted under 1.2 the DPS transducer was limited to ± 5 kPa, which constrained the altitude excursion to ± 550 m at 3000 m altitude and to ± 1000 m at 8400 m altitude.
- Limitations of the pressure reference vessel: Since sudden pressure changes would upset the temperature stability inside the reference vessel, it was decided to start and finish the accelerated run in steady level flight at approximately the same altitude.

In figure 5 and 6 the altitude and air speed variation during a typical accelerated run is shown. The following phases can be distinguished:

1. Steady level flight at the required altitude at a speed of approximately 1.3 V_S.
2. Engine stabilization with a duration of at least 30 seconds, the increased engine power is used to gain altitude at a slightly decreasing airspeed.
3. Measurement interval during which the aircraft is accelerated from 1.1 V_S to maximum speed at a rate of 0.5 ms^{-1} per second.
4. Return to initial altitude in preparation for the next run.
5. Steady level flight as required for DRUM.

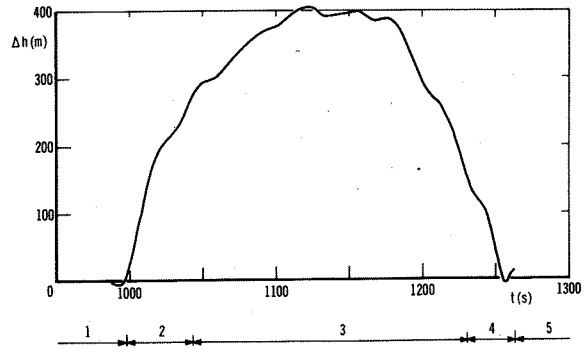

FIG. 5 ALTITUDE VARIATION

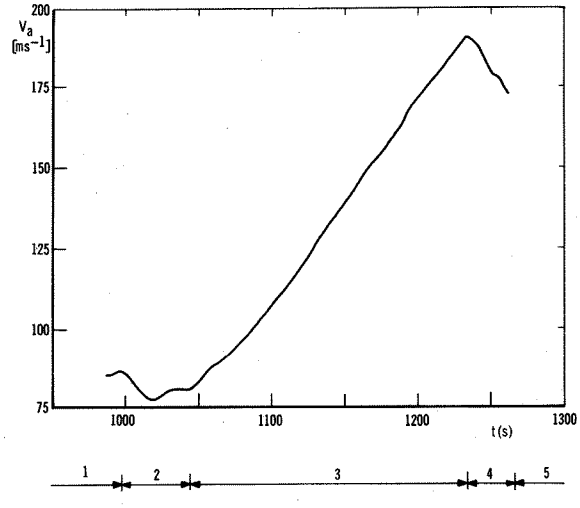

FIG. 6 AIRSPEED VARIATION

2.2 Pitch Excitations. In order to determine the aerodynamic model of the aircraft for symmetric flight a high frequency excitation of the pitch dynamics using the elevator is necessary.

The optimal elevator input signal was calculated with a program provided by Delft University of Technology. The elevator signal had to be flown by the pilot which limited the complexity and the duration. Therefore, the elevator signal was optimized for only a limited set of coefficients.

It turned out that, within the above constraint, the optimal signal for all flight conditions had the same general appearance, shown in Figure 7. The only difference was the total duration of the signal, which varied from 4 to 11 seconds.

The elevator input signal was practised on the NLR Moving Base Simulator. The pilot was provided with a simple control-stick deflection indicator,

marked only with the maxima and minima of the signal.
The result of the simulator trials was that it took some time before the pilot achieved the correct signal duration. Therefore, during the actual flight trials, the pilot was allowed to exercise several times before the recording of the data was started. During the recording a total of 5 pitch excitations were performed.

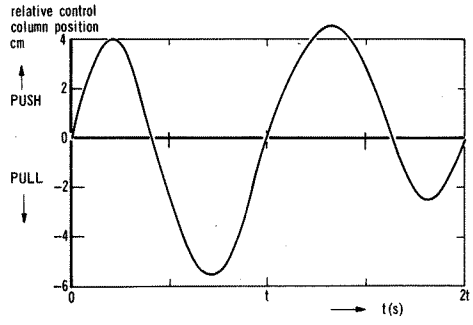

FIG. 7 ELEVATOR INPUT SIGNAL

2.3 Flight Test Program. For a realistic evaluation of the dynamic flight test technique a flight test program was defined, which contained many of the more important features of a complete certification program. Table 2 provides an overview of the flight test program, which was actually flown. It comprised 4 basic aircraft configurations, "clean", slats out, slats out + 25° flaps and slats out + 42° flaps.

For each configuration a series of pitch excitation measurements were performed in order to obtain necessary data for the aerodynamic model.

For each configuration a series of 7 measurements in steady flight ("partial climbs") were performed, for the clean configuration also for two different altitudes.

For each configuration a series of 5 accelerated runs were performed, distributed over two different flights. For the clean configuration a series of 3 accelerated runs were performed for 7 different flight conditions, in particular engine setting ($N_H/\sqrt{T_t}$), center of gravity (c.g.), altitude (FL 100,220 and 280) and load distribution. In addition 3 combined maneuvers, as originally developed by Delft University of Technology, were performed.

The first flight was dedicated to the check out of the instrumentation and to the practice of the maneuvers. The following two flights were dedicated to a determination of the Position Error Correction (PEC) of the "trailing cone" static tube. The actual flight tests were executed in 5 flights.

The complete flight program including the PEC and instrumentation checkout flights was executed within the allotted flight time of 20 hours. The last four measurement flights were executed in a one week period.

TABLE 2 FLIGHT TEST PROGRAM (5 flights)

Configuration	Partial climbs	Acc. runs	Pitch Exitations	Combined Maneuver
clean	13	29	5	3
slats out	7	5	4	-
slats out + flaps 25°	7	5	3	-
slats out + flaps 42°	-	3	-	-

3. Flight path reconstruction

3.0 Introduction. An essential part of the determination of aircraft performance from dynamic maneuvers is the flight path reconstruction. This flight path reconstruction supplies accurate time histories of the velocity components in three dimensions (u), (v), (w), the yaw angle (ψ), the pitch angle (θ), the bank angle (ϕ) and the altitude variation (Δh). The velocity components and the pitch and yaw angle cannot be measured satisfactorily in a direct way, even in the case of symmetric flight[8].

Prior to the flight path reconstruction the asymmetric motion of the aircraft has to be modelled in an equation of state. This equation describes the physical relationship between the seven given state components in terms of their time derivatives.

Moreover the control must be modelled. In principle the control consists of the accelerations in three dimensions (Ax, Ay, Az) and the three angular velocities (p, q, r). See also Fig 8.

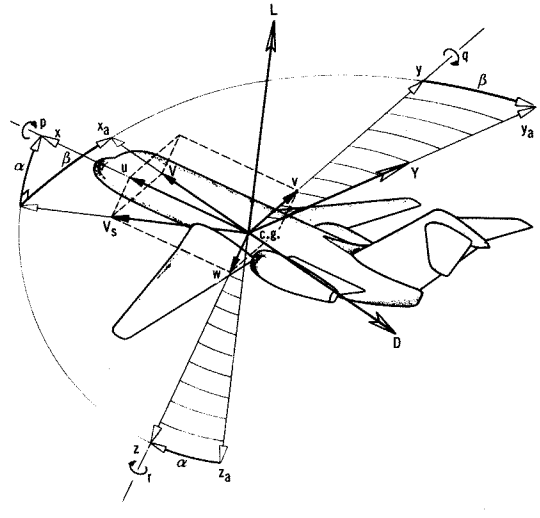

FIG. 8 BODY-FIXED REFERENCE AXIS (x, y, z) AND AIR-TRAJECTORY REFERENCE AXIS (x_a, y_a, z_a)

If the initial state, and the control as a function of time, were known, integration of the equation of state gives at each time the exact state and as an immediate result relevant quantities such as the angle of attack (α). In a physical

environment those quantities are corrupted with noise. In general zero shift and random errors have to be taken into account. The additional information, required for removal of these errors, may be obtained by recording the airspeed (Va), the altitude with respect to the altitude at the beginning of the dynamic manoevre (Δha), the slip angle (β) and the bank angle (ϕ). These quantities are simple algebraïc functions of the state components, however corrupted with noise.

The flight path reconstruction has now been formulated in terms of the combined estimation of the state (u), (v), (w), (ψ), (θ), (ϕ), (Δh) and the zero shifts (in principle six). This estimation problem can be solved with various methods[9]. Here the square root information formulation of the classic Kalman filter/smoother has been used. Theoretical and practical investigations show that this formulation is, though theoretically equivalent, numerically superior to the conventional formulation[10][11].

The following sections deal with the description of the system model, the linearization and discretization of this model into a form suitable for the application of the Kalman filter/smoother, the description of the square root information formulation of the Kalman filter/smoother, and the calculation of relevant flight path parameters such as flight path angle (γ) and angle of attack (α) from the estimated state.

3.1 The system model. Ignoring coriolis- and centrifugal forces the motion of the aircraft over a flat and non-rotating earth is described by the following set of equations[12]

$$\begin{aligned}
\dot{u} &= Ax - g\sin\theta - q.w + r.v \\
\dot{v} &= Ay + g\cos\theta\sin\phi - r.u + p.w \\
\dot{w} &= Az + g\cos\theta\cos\phi - p.v + q.u \\
\dot{\psi} &= q\sec\theta\sin\phi + r\sec\theta\cos\phi \\
\dot{\theta} &= q\cos\phi - r\sin\phi \\
\dot{\phi} &= p + q\sin\phi\tan\theta + r\cos\phi\tan\theta \\
\dot{\Delta h} &= u\sin\theta - v\sin\phi\cos\theta - w\cos\phi\cos\theta
\end{aligned} \tag{3.1}$$

In these equations the vector $\underline{X}$, defined by

$$\underline{X} = \text{col}\,(u,v,w,\psi,\theta,\phi,\Delta h) \tag{3.2}$$

is considered to be the state, while the vector $\underline{U}$, defined by

$$\underline{U} = \text{col}\,(Ax,Ay,Az,p,q,r) \tag{3.3}$$

is considered to be the input.
The equation of state of the aircraft can now be written in the usual form of a non linear vector differential equation

$$\dot{\underline{X}} = \underline{f}(\underline{X},\underline{U}) \tag{3.4}$$

$$\underline{X}(t_o) = \underline{X}_o \tag{3.5}$$

The equations (3.4) and (3.5) cannot be used for straight forward integration to reconstruct the state due to several reasons e.g.

- the initial state $\underline{X}_o$ is not known exactly
- the input signals are corrupted with noise
- the input signals contain (constant) zero-shifts
- the effect of coriolis- and centrifugal forces is not included
- the influence of atmospheric pertubations is not modelled

It will now be discussed how the system model can be modified, in order to account for these effects.

In view of the application of the Kalman filter/smoother the initial state is considered to be a stochastic variable, modelled by its expectation and covariance. Numerical values are obtained by maximum likelihood estimation on the initial 3 seconds period of an observation sequence. The input signals are modelled by the equation

$$\underline{U} = \underline{U}_m + \underline{\lambda} + \underline{w} \tag{3.6}$$

where $\underline{\lambda}$ represents the unknown zeroshift, which is assumed to be constant, and $\underline{w}$ is a random error assumed to be gaussian noise. As a consequence the state vector must be augmented with the vector $\underline{\lambda}$ for which the equation of state is

$$\dot{\underline{\lambda}} = 0 \tag{3.7}$$

In principle six components must be considered, but because of nominally symmetric flight the zero shifts in Ay and p can be discarded as being insignificant.

The effect of coriolis- and centrifugal forces is taken into account by inclusion of the following terms into the equations (3.10-3.16).

$$\begin{aligned}
Ax' &= Ax - A_x^c \\
Ay' &= Ay - A_y^c \\
Az' &= Az - A_z^c \\
p' &= p - p^c \\
q' &= q - q^c \\
r' &= r - r^c
\end{aligned} \tag{3.8}$$

The influence of atmospheric pertubations is not included in the system model, since test flights are normally performed under good weather conditions i.e. atmosphere in rest.

In addition to the measured input signals the vector

$$\underline{M} = \text{col}\,(Va,\Delta ha,\beta,\phi) \tag{3.9}$$

is measured during the flight. This output vector is corrupted with random errors, assumed to be gaussian noise.

Incorporation of equations (3.6)-(3.8) into (3.1) yields the system model for (a)symmetric flight over a rotating earth

$$\dot{u} = (Ax'+\lambda x) - g\sin\theta - (q'+\lambda_q)w + (r'+\lambda_r)v \tag{3.10}$$

$$\dot{v} = Ay' + g\cos\theta\sin\phi - (r'+\lambda_r)u + p'w \tag{3.11}$$

$$\dot{w} = (Az'+\lambda_z) + g\cos\theta\cos\phi - p'v + (q'+\lambda_q)u \tag{3.12}$$

$$\dot{\psi} = (q'+\lambda_q)\sec\theta\sin\phi + (r'+\lambda_r)\sec\theta\cos\phi \tag{3.13}$$

$$\dot{\theta} = (q'+\lambda_q)\cos\phi - (r'+\lambda_r)\sin\phi \tag{3.14}$$

$$\dot{\phi} = p' + (q'+\lambda_q)\sin\phi\tan\theta + (r'+\lambda_r)\cos\phi\tan\theta \tag{3.15}$$

$$\dot{\Delta h} = u\sin\theta - v\sin\phi\cos\theta - w\cos\phi\cos\theta \tag{3.16}$$

$$\dot{\lambda}_x = 0$$
$$\dot{\lambda}_z = 0 \qquad (3.17)$$
$$\dot{\lambda}_q = 0$$

Defining the augmented state vector $\underline{Y}$,

$$\underline{Y} = \text{col}\ (u,v,w,\psi,\theta,\phi,\Delta h,\lambda_x,\lambda_z,\lambda_q) \qquad (3.18)$$

and the unshifted input vector $\underline{U}^*$

$$\underline{U}^* = \underline{U} - \underline{\lambda} \qquad (3.19)$$

the sytem equations (3.10)-(3.17) can be written in the form

$$\dot{\underline{Y}} = \underline{f}(\underline{Y},\underline{U}^*) \qquad (3.20)$$
$$\underline{Y}\ (t_o) = \underline{Y}(o) \qquad (3.21)$$
$$\underline{M} = \underline{h}(\underline{Y}) + \underline{v} \qquad (3.22)$$

3.2 Linearization and discretization. In order to apply the linear Kalman filter/smoother the equations (3.20) and (3.22) must be linearized around a nominal trajectory $\underline{Y}_{nom}(t)$ and subsequently discretized. This nominal trajectory is computed by integration of

$$\dot{\underline{Y}}_{nom} = \underline{f}(\underline{Y}_{nom},\underline{U}^*_{nom}) \qquad (3.23)$$

over a segment of finite length between successive measurements. The initial conditions are for each step updated with the output signal $\underline{M}$. The input signal $\underline{U}^*_{nom}$ is taken as $\underline{U}_m - \underline{\lambda}_k$ ($\underline{\lambda}_k$ is an estimation based on k measurements). The correction for the state deviation is defined by

$$\underline{y}(t) = \underline{Y}(t) - \underline{Y}_{nom}(t) \qquad (3.24)$$

and for the input deviation by (see (3.6),(3.19))

$$\underline{u}(t) = \underline{U}^*(t) - \underline{U}^*_{nom}(t) = \underline{w}(t) \qquad (3.25)$$

Linearization of equation (3.20) around the nominal trajectory $\underline{Y}_{nom}$, $\underline{U}^*_{nom}$ leads to the linear equation

$$\dot{\underline{y}}(t) \simeq \left[\frac{\partial \underline{f}}{\partial \underline{Y}}\bigg|_{\underline{Y}=\underline{Y}_{nom}}\right] y(t) + \left[\frac{\partial \underline{f}}{\partial \underline{U}}\bigg|_{\underline{U}=\underline{U}^*_{nom}}\right] .\underline{w}(t) \qquad (3.26)$$

The correction for the output deviation is defined by

$$\begin{aligned}\underline{m}(t) &= \underline{M}(t) - \underline{M}_{nom}(t)\\ &= \underline{h}(\underline{Y}) + \underline{v}(t) - \underline{h}(\underline{Y}_{nom})\\ &\simeq \left[\frac{\partial \underline{h}}{\partial \underline{Y}}_{\underline{Y}=\underline{Y}_{nom}}\right] .\underline{y}(t) + \underline{v}(t)\end{aligned} \qquad (3.27)$$

The equations (3.26) (3.27) can be rewritten in the symbolic form

$$\begin{aligned}\dot{\underline{y}}(t) &= \begin{bmatrix} A & B \\ 0 & 0 \end{bmatrix} \underline{y}(t) + \begin{bmatrix} B \\ 0 \end{bmatrix} \underline{w}(t)\\ \underline{m}(t) &= H.\ \underline{y}(t) + \underline{v}(t)\end{aligned} \qquad (3.28)$$

Discretization of equation (3.28) yields the system

$$\begin{aligned}\underline{y}_{k+1} &= \phi_{k+1,k}\ \underline{y}_k + \Gamma_{k+1,k} \cdot \underline{w}_k\\ \underline{m}_k &= H_k \cdot \underline{y}_k + \underline{v}_k\end{aligned} \qquad (3.29)$$

For further details on the relation between $\phi_{k+1,k}$, $\Gamma_{k+1,k}$, H_k and $f(\underline{Y},\underline{U}^*)$ and $h(\underline{Y})$ the reader is referred to standard textbooks on modern control theory.(13)(14)

The equations (3.29) are in a form suitable for the application of a discrete Kalman filter. Since the nominal trajectory $\underline{Y}_{nom}$ is updated with the measurements $\underline{M}$ the validity of the linear equations (3.29) as perturbations equations is garantueed. An inherent problem when using a Kalman filter/smoother is the modelling of system noise $\underline{w}_k$ and measurements noise $\underline{v}_k$. Calibration results have been used for estimation of the covariance matrices. The validity of this noise modelling has been checked against the statistics of the measurements residuals with satisfactory results.

3.3 The square root information filter/smoother. Consider a system described by (3.29) as a linearization around a nominal trajectory $\underline{Y}_{nom}$ as described in section 3.2. A Kalman filter estimates the state $\underline{y}_{k+1}$ from the state $\underline{y}_k$ according to a two-step update procedure

(i) time update, based on the system dynamics
(ii) measurements update, based on the measurements

As a result of the chosen nominal trajactory $\underline{Y}_{nom}$ the estimate $\hat{\underline{y}}_k$, based on measurements up to t_k, equals zero. Consequently the time update $\tilde{\underline{y}}_{k+1}$ equals zero. (See equation (3.29)). Let Λ_k, Λ_w, Λ_v be the covariance matrices of respectively $\underline{y}_k$, $\underline{w}_k$, $\underline{v}_k$ and let R_k, R_w and R_v be defined by

$$R_k R_k^T = \Lambda_k^{-1} \qquad (3.30)$$
$$R_w R_w^T = \Lambda_w^{-1} \qquad (3.31)$$
$$R_v R_v^T = \Lambda_v^{-1} \qquad (3.32)$$

The time update $\tilde{R}_{k+1}$ (defining $\tilde{\Lambda}^{-1}_{k+1} = \tilde{R}_{k+1}\tilde{R}^T_{k+1}$) follows from

$$T_1 \begin{bmatrix} R_w & 0 \\ \hat{R}_k\ \phi^{-1}_{k+1,k}\Gamma_{k+1,k} & \hat{R}_k\ \phi^{-1}_{k+1,k} \end{bmatrix} = \begin{bmatrix} R'_{k+1} & R''_{k+1} \\ 0 & \tilde{R}_{k+1} \end{bmatrix} \qquad (3.33)$$

where T_1 is a householder matrix (15) to ensure that $\tilde{R}_{k+1}$ is an upper triangular matrix.

The measurements update from $\tilde{\underline{y}}_{k+1}$ to $\hat{\underline{y}}_{k+1}$ is defined by

$$T_2 \begin{bmatrix} 0 \\ R_v\ \underline{m}_{k+1} \end{bmatrix} = \begin{bmatrix} \hat{\underline{d}}_{k+1} \\ \underline{d}' \end{bmatrix} \qquad (3.34)$$

The measurement update from $\tilde{R}_{k+1}$ to $\hat{R}_{k+1}$ is defined by

$$T_2 \begin{bmatrix} \tilde{R}_{k+1} \\ R_v\ H_{k+1} \end{bmatrix} = \begin{bmatrix} \hat{R}_{k+1} \\ 0 \end{bmatrix} \qquad (3.35)$$

The matrix T_2 which is used in the equations (3.34) and (3.35) is a householder matrix to ensure that $\hat{R}_{k+1}$ is upper triangular. The correction $\hat{\underline{y}}_{k+1}$ can be calculated from

$$\hat{R}_{k+1} \cdot \hat{\underline{y}}_{k+1} = \hat{\underline{d}}_{k+1} \qquad (3.36)$$

After an update of Y_{nom} with $\hat{y}_{k+1}$ from equation (3.36) $\underline{\hat{y}}_{k+1}$ becomes zero and the next step in the filter procedure can proceed.

Summarizing

The square root information filter works with the square root information matrix R_k instead of the actual covariance matrix Λ_k. Calculation of $\underline{\hat{y}}_{k+1}$ and $\hat{R}_{k+1}$ from $\hat{y}_k$ and $\hat{R}_k$ goes along the following steps:

$$\begin{array}{ccccc} \hat{R}_k & \xrightarrow{(3.33)} & \tilde{R}_{k+1} & \xrightarrow{(3.35)} & \hat{R}_{k+1} \\ \underline{\hat{y}}_k & \xrightarrow{(3.29)} & \underline{\tilde{y}}_{k+1} & \xrightarrow{(3.34)} & \underline{\hat{d}}_{k+1} \quad \xrightarrow{(3.36)} \quad \underline{\hat{y}}_{k+1} \\ & & & & \underline{m}_{k+1} \end{array} \tag{3.37}$$

After a complete filtering of the state $\underline{y}_k$ estimates $\underline{\hat{y}}_k$ and corresponding square root information matrices $\hat{R}_k$ are known. For each state estimation $\underline{\hat{y}}_k$ holds that it is based upon measurements prior and up to t_k. It is possible to improve the estimation of $\underline{y}_k$ by application of the "square root information fixed interval smoother", which produces estimates $\underline{\check{y}}_k$ based on all measurements. These estimates are calculated backwards since

$$\underline{\check{y}}_{kmax} = \underline{\hat{y}}_{kmax} \tag{3.38}$$

$$\check{R}_{kmax} = \hat{R}_{kmax} \tag{3.39}$$

Let the estimates $\underline{\check{y}}_{k+1}$ and $\check{R}_{k+1}$ be given. It will now be described how the estimates $\underline{\check{y}}_k$ and $\check{R}_k$ can be calculated. The matrix $\check{R}_k$ follows from the householder transformation (R'_{k+1} and R''_{k+1} are defined in eq. 3.33).

$$T_3 \begin{bmatrix} R'_{k+1} + R''_{k+1} \cdot \Gamma_k & R''_{k+1} \phi_k \\ \check{R}_{k+1} \Gamma_k & \check{R}_{k+1} \phi_k \end{bmatrix} = \begin{bmatrix} R'''_k & R''''_k \\ 0 & \check{R}_k \end{bmatrix} \tag{3.40}$$

The measurements update $\underline{\check{y}}_k$ is defined by

$$T_3 \begin{bmatrix} 0 \\ \check{R}_{k+1} \quad \underline{\check{y}}_{k+1} \end{bmatrix} = \begin{bmatrix} d \\ \underline{\check{d}}_k \end{bmatrix} \tag{3.41}$$

$$\check{R}_k \, \underline{\check{y}}_k = \underline{\check{d}}_k \tag{3.42}$$

The smooth estimate of $\underline{Y}_k$ is given by

$$\underline{\check{Y}}_k = \underline{\tilde{y}}_k + \underline{\check{y}}_k \tag{3.43}$$

with covariance matrix $\check{\Lambda}_k = R_k^{-1} R_k^{-T}$, (3.44)

where $\tilde{Y}_k = Y_{nom,k} + \tilde{y}_k$

Summarizing

The square root information smoother requires intermediate results from the square root information filter. Calculation of $\underline{\check{y}}_k$ and $\check{R}_k$ from $\underline{\check{y}}_{k+1}$ and R_{k+1} goes along the following steps:

$$\begin{array}{ccccc} \check{R}_{k+1} & \xrightarrow{(3.40)} & \check{R}_k & & \\ \underline{\check{y}}_{k+1} & \xrightarrow{(3.41)} & \underline{\check{d}}_k & \xrightarrow{(3.42)} & \underline{\check{y}}_k \end{array} \tag{3.45}$$

3.4 Calculation of angle of attack and related quantities. The angle of attack α is related to the velocity components w and u by the formula

$$\alpha = \text{arctg} \, \frac{w}{u} \tag{3.46}$$

The time derivative $\dot{\alpha}$ can be found by numerical differentiation of the angle α according to

$$\dot{\alpha}_i = 16 \left[\frac{1}{12} \alpha_{i-2} - \frac{2}{3} \alpha_{i-1} + \frac{2}{3} \alpha_{i+1} - \frac{1}{12} \alpha_{i+2} \right] \tag{3.47}$$

The flight path angle γ is related to the velocity components by the formula

$$\gamma = \arcsin \frac{u \sin\theta - w \cos\phi\cos\theta - v \sin\phi\cos\theta}{V} \tag{3.48}$$

where the numerator represents the climb velocity and V the overall velocity.

For the identification of the aerodynamic model coefficients the dimensionless aerodynamic coefficients C_x, C_z and C_m are defined as[12]

$$C_x = \frac{W \cdot (A_x + \lambda_x)}{\frac{1}{2} \rho V^2 . S}$$

$$C_z = \frac{W \cdot (A_z + \lambda_z)}{\frac{1}{2} \rho V^2 . S} \tag{3.49}$$

$$C_m = \frac{I_y \cdot \dot{q}}{\frac{1}{2} \rho V^2 . S . \bar{c}}$$

The quantities λ_x, λ_z and V are results of the flight path reconstruction. I_y, W, S and $\bar{c}$ are aircraft dependent constants. (See also section 4.4).

4. Aerodynamic model identification and calculation of aircraft performance characteristics

4.0 Introduction. Accurate flightpath reconstruction yields time histories of quantities like

α	angle of attack
M	Mach number
$\dot{\alpha}$	time derivative of angle of attack
q	rate of pitch
δ_e	elevator angle
δ_h	stabilizer angle

(4.01)

Aerodynamic model identification starts with the assumption that a relatively simple (e.g. polynomial) model based on the above given parameters gives a good description of the quantities C_x^*, C_z^* and C_m^*. These are quantities related to the resultant aerodynamic force along the appropriate axis. The engine thrust plays of course a central role in the definition of these quantities. If TE is the nett engine thrust, then C_x^*, C_z^* and C_m^* are defined by

$$C_x^* = C_x - \frac{TE \cdot \cos i_p}{\frac{1}{2} \rho V^2 S} \tag{4.02}$$

$$C_z^* = C_z - \frac{TE \cdot \sin i_p}{\frac{1}{2}\rho V^2 S} \qquad (4.03)$$

$$C_m^* = C_m - \frac{a \cdot TE}{\frac{1}{2}\rho V^2 S\bar{c}} \qquad (4.04)$$

Here i_p,S etc. are aircraft geometry dependent constants. (See also section 4.4).

The complexity of the model is somewhat arbitrary. In general the type of aircraft under consideration as well as the class of dynamic maneuvers should determine the actual model. The flight maneuvers mentioned in section 2 each require a typical model. For ease of calculations a general model, which encompasses all particular models, is chosen. The coefficients in this model are calculated by minimizing the squared residual sum, thus

$$\min_{\underline{c}} \left\{ C_x^* - f(\alpha, M, \dot{\alpha}, q, \delta_e, \delta_h; \underline{c}) \right\}^2 \qquad (4.05)$$

After identification of the model coefficients vector $\underline{c}$ (for C_x^*, C_z^* and C_m^*) the calculation of performance characteristics can take place. Therefore the quantities $V_1, \theta_1, Cx_1, \delta e_1, \delta h_1$ which identify the dynamic flight condition have to be reduced to quantities $V_2, \theta_2, C_{x_2}, \delta_{e_2}, \delta_{h_2}$ corresponding to steady rectilinear ascending (descending) trimmed flight at a specified weight, center of gravity position and altitude, i.e. $\dot{u}_2 = \dot{w}_2 = q_2 = \dot{q}_2 = \delta_{e_2} = 0$[8]. From the equivalent steady flight quantities C_{x_2} and C_{z_2} the lift and drag coefficients C_L and C_D are easily calculated and, as a final result indicating the aircraft performance, the lift-drag polar. In the following sections it will be discussed how to calculate the aerodynamic model coefficients via an interactive adaptive procedure that combines the human intelligence and the calculation speed of a modern computer. The sensitivity of the various model coefficients will be discussed. The calculation of the "steady flight" quantities will be indicated as well as the calculation of the lift-drag polar. Detailed information about this interactive procedure can be found in the literature.[16][17][18]

4.1 Interactive identification of aerodynamic model coefficients. The general model consists of the following three equations for the quantities C_x^*, C_z^* and C_m^* as defined in section 4.0.

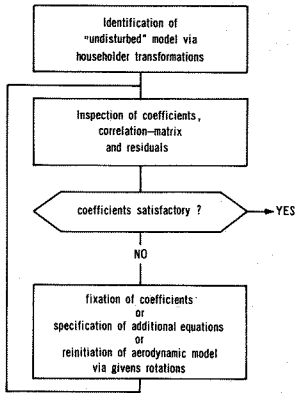

FIG. 9 INTERACTIVE IDENTIFICATION OF AERODYNAMIC MODEL COEFFICIENTS

$$(C_x^* \; C_z^* \; C_m^*) = \begin{bmatrix} 1 \\ \alpha \\ \alpha^2 \\ M \\ M^2 \\ \alpha M \\ \frac{\dot{\alpha}\bar{c}}{V} \\ \frac{q\bar{c}}{V} \\ \delta_e \\ \delta_h \end{bmatrix}^T \cdot \begin{bmatrix} C_{x_o} & C_{z_o} & C_{m_o} \\ C_{x_\alpha} & C_{z_\alpha} & C_{m_\alpha} \\ C_{x_{\alpha 2}} & C_{z_{\alpha 2}} & C_{m_{\alpha 2}} \\ C_{x_M} & C_{z_M} & C_{m_M} \\ C_{x_{M2}} & C_{z_{M2}} & C_{m_{M2}} \\ C_{x_{\alpha M}} & C_{z_{\alpha M}} & C_{m_{\alpha M}} \\ C_{x_{\dot{\alpha}}} & C_{z_{\dot{\alpha}}} & C_{m_{\dot{\alpha}}} \\ C_{x_q} & C_{z_q} & C_{m_q} \\ C_{x_{\delta_e}} & C_{z_{\delta_e}} & C_{m_{\delta_e}} \\ C_{x_{\delta_h}} & C_{z_{\delta_h}} & C_{m_{\delta_h}} \end{bmatrix} \qquad (4.05)$$

or symbolically AC = B

$$\begin{bmatrix} 1 & & \delta_h \\ & (A) & \\ 1 & & \delta_h \end{bmatrix} \begin{bmatrix} C_{x_o} & C_{z_o} & C_{m_o} \\ & (C) & \\ C_{x_{\delta_h}} & & C_{m_{\delta_h}} \end{bmatrix} = \begin{bmatrix} C_x^* & C_z^* & C_m^* \\ & (B) & \\ C_x^* & C_z^* & C_m^* \end{bmatrix} \qquad (4.06)$$

Each measurement produces a horizontal line in the matrices A and B and a rectangular matrix A of several hundred rows results from a dynamic maneuver. The equation AC = B is premultiplied by a householder matrix T such that TA = R is upper triangular. From the transformed system RC = TB the coefficients $C_{x_o} \ldots C_{m_{\delta_h}}$ follow straightforwardly.

The selected dynamic maneuvers supply the a priori knowledge that some of the coefficients cannot be identified but should be fixed in advance (sec.2). Fixation of coefficients has an (unknown) influence on the approximation power of the model if it is done in advance. By applying givens rotations[15] afterwards, this influence can be quantified. Storage of the matrix R (which requires a small amount of core storage!) opens the way to alternative fixations with approximately equal residuals sum. The interactive procedure as outlined in figure 9 turns out to be a very flexible tool for aerodynamic model identification.

4.2 Sensitivity analysis. In order to verify the validity of the chosen aerodynamic model a sensitivity analysis may be used. Model validation may include comparison with experiments and/or a priori knowledge and comparison of mathematical model with physical model. In this section however an isolated aspect of this validation will be discussed and to do that the sensitivity analysis will be defined in a precise mathematical setting.

Consider the matrix equation AC = B where A and B are results from measurements and/or flight reconstruction and C is a solution in least-squares sense. Since A and B result from measurements they are corrupted with noise. Let δA and δB be matrices such that $A + \delta A$ and $B + \delta B$ are matrices which could be the result of an equivalent

testflight. Thus δA and δB represent the noise upon A and B. Let C + δC be the solution in least-squares sense of (A + δA) (C + δC) $\simeq$ B + δB. The sensitivity analysis of this section deals with determination of the relation between δC, δA and δB[15].

Since the sensitivity analysis can be performed for each column of C separately this will be done and a slight change of notation will be used.
The following theorem has been proved [15]:

Let x be the minimum length solution to the least squares problem Ax $\simeq$ b with residual r = b - Ax. Assume $\|\delta A\| \cdot \|A^+\| \leq 1$ and rank (A + δA) $\leqslant$ rank (A). Let x + δx be the minimum length solution of the problem

$$(A + \delta A)(x + \delta x) \simeq b + \delta b$$

then one has

$$\text{(i)} \quad \text{Rank } (A + \delta A) = \text{Rank } (A) \tag{4.07}$$

$$\text{(ii)} \quad \frac{\|dx\|}{\|x\|} \leq \hat{\kappa} \left\{(2 + \kappa\rho)\alpha + \gamma\beta\right\}$$

Here A^+ denotes the pseudo inverse of a matrix A, $\|x\|$ the Euclidean length of a vector, $\|A\|$ the spectral matrix norm, κ the conditionnumber of A, $\alpha = \frac{\|\delta A\|}{\|A\|}$, $\beta = \frac{\|db\|}{\|b\|}$, $\gamma = \frac{\|b\|}{\|A\| \cdot \|x\|}$,

$\rho = \frac{\|r\|}{\|A\| \cdot \|x\|}$.

Thus the right hand side of equation (4.07) contains quantities, which can be calculated for a given least squares problem. If the right hand side is known the sensitivity of the solution x, as represented by δx can be calculated. The condition number κ is calculated by a singular value decomposition of A.

It is noted that none of the selected dynamic maneuvers of section 2 resulted in a matrix A with full pseudo rank which means that fixation of some parameters must take place to ensure $\|dx\| < \infty$. Based on an estimation of $\alpha = \beta = .001$ from calibration results, the pseudo rank of A turns out to be 4 or 5. Which parameters have to be fixed depends on the particular dynamic maneuver, but for the resulting free parameters a relative error of 1 up to 10 % was achieved.

4.3 Reduction to steady-state flight conditions. As stated in section 4.0 the steady flight to which the dynamic maneuver is reduced is the rectilinear ascending (descending) trimmed flight. ($\delta_{e_2} = 0$). Calculation of the quantities V_2, θ_2, C_{x_2}, C_{z_2}, δ_{h_2} requires the solution of the following set of equations[8]

$$C_{x_2} \cdot \tfrac{1}{2}\rho_2 V_2^2 \cdot S - W_2 g \sin\theta_2 = 0 \tag{4.08}$$

$$C_{z_2} \cdot \tfrac{1}{2}\rho_2 V_2^2 \cdot S + W_2 g \cos\theta_2 = 0 \tag{4.09}$$

$$\begin{aligned} C_{x_2} = {} & C_{x_1} + C_{x_M}\left(\frac{V_2}{\sqrt{\gamma RT_2}} - M_1\right) + C_{x_{M^2}}\left(\frac{V_2^2}{\gamma RT_2} - M_1^2\right) \\ & + C_{x_{\alpha M}}\left(\frac{\alpha_1 V_2}{\sqrt{\gamma RT_2}} - \alpha_1 M_1\right) - C_{x_{\dot\alpha}} \cdot \left(\frac{\dot\alpha_1 \cdot \bar c}{V_1}\right) \\ & - C_{x_q} \cdot \left(\frac{q_1 \cdot \bar c}{V_1}\right) - C_{x_{\delta_e}} \cdot \delta_{e_1} + C_{x_{\delta_h}}(\delta_{h_2} - \delta_{h_1}) \\ & + TE \cdot \left(\frac{\cos i_p}{\frac{1}{2}\rho_2 V_2^2 S} - \frac{\cos i_p}{\frac{1}{2}\rho_1 V_1^2 S}\right) \end{aligned} \tag{4.10}$$

$$\begin{aligned} C_{z_2} = {} & C_{z_1} + C_{z_M}\left(\frac{V_2}{\sqrt{\gamma RT_2}} - M_1\right) + C_{z_{M^2}}\left(\frac{V_2^2}{\gamma RT_2} - M_1^2\right) \\ & + C_{z_{\alpha M}}\left(\frac{\alpha_1 V_2}{\sqrt{\gamma RT_2}} - \alpha_1 M_1\right) - C_{z_{\dot\alpha}}\left(\frac{\dot\alpha_1 \cdot \bar c}{V_1}\right) \\ & - C_{z_q}\left(\frac{q_1 \cdot \bar c}{V_1}\right) - C_{z_{\delta_e}} \cdot \delta_{e_1} + C_{z_{\delta_h}}(\delta_{h_2} - \delta_{h_1}) \\ & + TE \cdot \left(\frac{\sin i_p}{\frac{1}{2}\rho_2 V_2^2 S} - \frac{\sin i_p}{\frac{1}{2}\rho_1 V_1^2 S}\right) \end{aligned} \tag{4.11}$$

$$\begin{aligned} -C_{m_{\delta_h}}(\delta_{h_2} - \delta_{h_1}) = {} & C_{m_1} + C_{m_M}\left(\frac{V_2}{\sqrt{\gamma RT_2}} - M_1\right) \\ & + C_{m_{M^2}}\left(\frac{V_2^2}{\gamma RT_2} - M_1^2\right) + C_{m_{\alpha M}}\left(\frac{\alpha_1 V_2}{\sqrt{\gamma RT_2}} - \alpha_1 M_1\right) \\ & - C_{m_{\dot\alpha}}\left(\frac{\dot\alpha_1 \cdot \bar c}{V_1}\right) - C_{m_q}\left(\frac{q_1 \cdot \bar c}{V_1}\right) - C_{m_{\delta_e}} \cdot \delta_{e_1} \\ & - C_{z_2}\left(\frac{X_{cg_2} - X_{cg_1}}{\bar c}\right) + C_{x_2}\left(\frac{Z_{cg_2} - Z_{cg_1}}{\bar c}\right) \\ & + (Z_{c_{g_1}} + .434 - .03\, X_{c_{g_1}}) \cdot \frac{TE}{\bar c} \cdot \left(\frac{1}{\frac{1}{2}\rho_2 V_2^2 S} - \frac{1}{\frac{1}{2}\rho_1 V_1^2 S}\right) \end{aligned} \tag{4.12}$$

Equations (4.08), (4.09) are solved for V_2 and θ_2 in terms of C_{x_2} and C_{z_2}. The equation for V_2 becomes

$$V_2 = \sqrt{\frac{W_2 \cdot g}{\frac{1}{2}\rho_2 S \sqrt{C_{x_2}^2 + C_{z_2}^2}}} \tag{4.13}$$

The equations (4.10) and (4.11) are substituted into the equations (4.12) and (4.13) The latter two equations now form a system of two nonlinear equations in two unknowns V_2 and δ_{h_2}. This system has a Jacobian with determinant of order 1 and is therefore solved with Newton-Raphson iteration. C_{x_2} and C_{z_2} are calculated from equations (4.10) and (4.11) and θ_2 follows from

$$\theta_2 = \text{arctg}\left(-\frac{C_{x_2}}{C_{z_2}}\right) \tag{4.14}$$

As initial values for V_2 and δ_{h_2} the values V_1 and δ_{h_1} are chosen. A solution with relative accuracy of .0001 was reached in 3 steps on the average.

4.4 Calculation of lift-drag polar. The quantities C_{x_2} and C_{z_2} as a result of the reduction procedure described in section 4.3 can be transformed into the lift and drag coefficients C_L and C_D via transformation from the body-fixed reference system to the air trajectory reference system.

If K_{x_a} and K_{z_a} are the forces acting on the aircraft in the X and Z dimension then the

following relations hold

$$K_{x_a} = (TE \cos i_p)\cos\alpha\cos\beta + (TE \sin i_p)\sin\alpha\cos\beta - D \quad (4.15)$$

$$K_{z_a} = (TE \cos i_p)\sin\alpha - (TE \sin i_p)\cos\alpha - L \quad (4.16)$$

Here α is the angle of attack, β is the slip angle and i_p is the angle between the direction of TE and the X-axis of the body-fixed reference system.

These forces are related to the accelerations Ax, Ay and Az via the equations

$$K_{x_a} = W_2 (Ax \cos\alpha\cos\beta + Ay \sin\beta + Az \sin\alpha\cos\beta) \quad (4.17)$$

$$K_{z_a} = W_2 (-Ax \sin\alpha + Az \cos\alpha) \quad (4.18)$$

Substitution of (4.17) and (4.18) into (4.15) and (4.16) and division by $\frac{1}{2}\rho_2 V_2^2 S$ yields for C_L and C_D

$$C_D = \frac{TE}{\frac{1}{2}\rho_2 V_2^2 S}(\cos i_p \cos\alpha\cos\beta + \sin i_p \sin\alpha\cos\beta) - C_{x_2}\cos\alpha\cos\beta - \frac{W_2 A_y}{\frac{1}{2}\rho_2 V_2^2 S}\sin\beta - C_{z_2}\sin\alpha\cos\beta \quad (4.19)$$

$$C_L = \frac{TE}{\frac{1}{2}\rho_2 V_2^2 S}(-\cos i_p \sin\alpha + \sin i_p \cos\alpha) + C_{x_2}\sin\alpha - C_{z_2}\cos\alpha \quad (4.20)$$

5. Preliminary Results

During the flight test program a total of 27 partial climbs, 45 accelerated runs and 60 pitch rotations were executed for 11 different combinations of aircraft configurations and flight conditions. Only a few results will be presented in this paper.

5.1 Flight Path Reconstruction. Since the actual flight path is unknown, it is difficult to evaluate the flight path reconstruction results. Therefore, this procedure was applied to simulated data in order to verify the correct reconstruction of the flight path. In practice, the residues, $\Delta\Delta h$ and ΔV, will virtually always be made to conform to the predicted statistics by the action of the Kalman filter.

The a priori statistics for Δh and V were chosen at slightly pessimistic values of 1 m and 1 ms^{-1} respectively, in order to account for the fact that the errors in the air data measurements are coloured. Figures 10 and 11 show a typical result for these parameters. The influence of pitch excursions on the residues is apparent.

As described earlier a complete six degree of freedom flight path reconstruction was implemented. Early experiments showed the necessity of adding an extra measurement to Δh and V in order to bound the unobservable angle of side slip β. Therefore, a side slip vane was mounted on the nose boom of the F 28. The accuracy of the β-reconstruction has very little influence on the accuracy of the α-reconstruction.

Small errors in the flight path reconstruction are readily apparent in the lift-drag polars. For example, some deviations in the lift-drag polars were traced to incorrect values of the delays in the pitot-static system. Therefore, the quality of the lift-drag polars are the ultimate test for the flight path reconstruction.

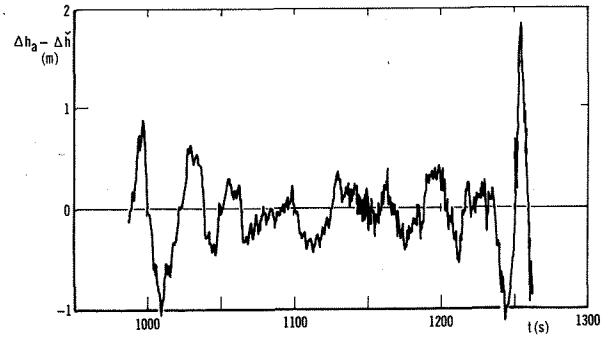

FIG. 10 RESIDUE OF THE ALTITUDE VARIATION

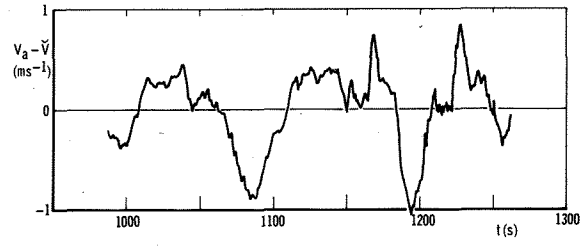

FIG. 11 RESIDUE OF AIRSPEED

5.2 Lift-Drag Polars. In this section some results are presented for the clean configuration at an altitude of 3000 m (FL 100). Since an aerodynamic model is required for the reduction to

steady-state flight conditions, this will be discussed first.

On the basis of the pitch excitations measurements as well as the accelerated runs an aerodynamic model for the clean aircraft configuration has been determined. A first result from the analysis in 4.2 was that not all parameters which were initially chosen were identifiable. Therefore, some selected parameters were fixed at a zero value. The residues of the simplified model did not increase significantly.

On the basis of data supplied by Fokker-VFW, an a priori aerodynamic model was defined. Some of the coefficients of the model based on the measurements deviated significantly from the a priori model, however use of either model in the reduction to steady-state flight conditions had a negligeable effect on the resulting lift-drag polars.

Since the (C_L, C_D) data pairs conform reasonably well to a second degree poly-nominal, the data from each run was fitted with the equation:

$$C_D = C_{D_{o_i}} + \beta'_i \cdot C_L^2 \qquad i = 1,..4$$

Subsequently the average values $\overline{C_{D_o}}$ and $\overline{\beta'}$ over the 4 runs were calculated. Table 3 presents the deviations of $C_{D_{o_i}}$ and β'_i from $\overline{C_{D_o}}$ and $\overline{\beta'}$ for each run expressed as a percentage of $\overline{C_{D_o}}$ and $\overline{\beta'}$ respectively. In addition table 3 presents the sample standard deviations, also expressed as a percentage of $\overline{C_{D_o}}$ and $\overline{\beta'}$.

	C_{D_o}	β'
run 1	+ 0,9 %	+ 1,2 %
run 2	- 4,0 %	+ 3,4 %
run 3	+ 0,4 %	- 0,6 %
run 4	+ 2,7 %	- 4,2 %
sample s.d. all runs	$S_{C_{D_o}}$ = 2,8 %	$S_{\beta'}$ = 3,2 %
sample correlation coefficient	$r_{C_{D_o},\beta}$ = -0,88	

TABLE 3 RESULTS FOR PARAMETERS C_{D_o} AND β'

It is clear that the calculated values of C_{D_o} and β' are strongly correlated (sample correlation coefficient $r_{C_{D_o},\beta} = -0,88$). In Figure 12 the curve corresponding to

$$C_D = C_{D_o} + \beta' \cdot C_L^2$$

is shown, together with the 2 s.d. error bounds calculated form the sample standard deviations and correlation coefficient. The estimated standard deviation varies from a minimum of 1,4 % at intermediate values of C_L to 1,8 % at low values of C_L and 2,1 % at high values of C_L.

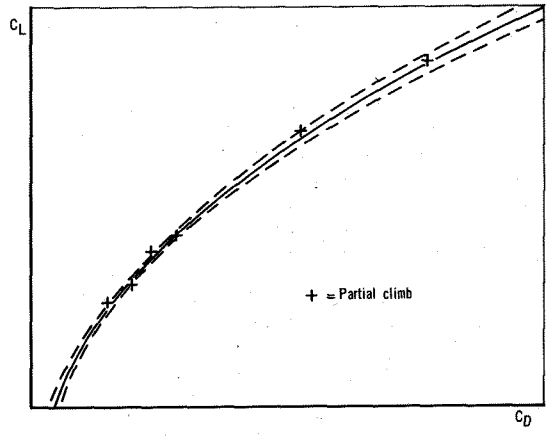

FIG. 12 LIFT - DRAG POLAR

In the same figure the results of the measurements in steady flight (partial climbs) are presented. The data points do not deviate systematically from the result of the accelerated runs. In addition, the scatter in the data points is comparable to the estimated error bounds.

6. Conclusions

In this paper a short overview has been given of a method to extract performance data from dynamic maneuvers for a jet transport aircraft. From the flight test program and subsequent data processing the following conclusions can be drawn

(i) A highly accurate instrumentation system has been built and has been used succesfully in the described flight test program.

(ii) Data processing of complex data structures is possible within an acceptable time span. Although special software has been developed for flight path reconstruction and aerodynamic model identification application of this software is straightforward on a medium size computer (Cyber 7213 with 64 K memory).

(iii) Preliminary results of the dynamic flight test technique show an accuracy within the limits of the steady-state test technique.

(iv) Stability and control parameters (aerodynamic model) are a natural result of the dynamic flight test technique. Important parameters can be estimated with an accuracy of 1 %, while other parameters, depending on the particular maneuver, can be estimated with an accuracy of 10 %.

(v) Pilot opinion expresses no special problems for dynamic maneuvers as compared with the partial climbs of the steady-state test technique.

(vi) The gain in test flight hours is significant. For the steady-state test technique 15 partial climbs are normally used for a

reliable lift drag polar, while for the dynamic flight test technique 5 accelerated runs yield an equivalent confidence level. Taking into account the duration per measurement a 50 % decrease in flight time can be expected.

Acknowledgement:

The authors would like to acknowledge the support of many persons and organisations which made the carrying out of these tests possible. In particular our thanks go to the Fokker-VFW International Aircraft Factories for their active participation and to the department of Aerospace Engineering of the Delft University of Technology for their inspiration and support during the early phases of this project and finally to the National Aeronautics and Space Administration for the loan of the three rate gyroscopes, which were essential for the success of this project.

7. References

(1) Hussenot
Méthodes Nouvelles d'Essais en Vol,
Technique et Science Aeronautique, Vol 6,
pp 38-49, 1950

(2) Vleghert, J.P.K.
Measuring climb performance of a propeller engined transport aeroplane using the acceleration technique,
AGARD Report 127, 1957

(3) Gerlach, O.H.
Analyse van een mogelijke methode voor het meten van prestaties en stabiliteits- en besturingseigenschappen van een vliegtuig in niet-stationaire, symmetrische vluchten,
Delft University of Technology, Report VTH-117, 1964

(4) Gerlach, O.H.
The determination of stability derivatives and performance characteristics from dynamic maneuvers,
AGARD CP-85, 1971

(5) Mulder, J.A.
Estimation of drag and thrust of jet-propelled aircraft by non steady flight test maneuvers,
AGARD FMP Symposium on Flight Test Techniques, Porz-Wahn, October 1976

(6) Abbink, F.J.
A computer-controlled avionics-data acquisition system,
NLR MP 78004 U, 1978

(7) Joosten, L.J.M.
Determination of performance and stability characteristics from dynamic longitudinal maneuvers with the Fokker F28 transport aircraft; description of the inertial strap-down system,
NLR TR 78058 U

(8) Jonkers, H.L. and Mulder, J.A.
Accuracy limits in nonsteady flight testing,
ICAS paper 76-46. Ottawa, Canada, 1976.

(9) Traas, C.R.
Digital filtering methods with applications to satellite altitude determination in the presence of modelling errors, Vol I,
NLR TR 76048 C

(10) Kaminski, P.G. et. al.
Discrete square-root filtering: A survey of current techniques,
IEEE transactions on automatic control, vol. AC-16, no. 6, December 1971

(11) Van de Wilt, M.
Flight-path reconstruction of symmetric nonsteady flights,
NLR TR 76133 U

(12) Jonkers, H.L.
Application of the Kalman filter to flight path reconstruction from flight test data including estimation of instrumental bias error corrections,
Ph.D. thesis, Delft, the Netherlands, 1976

(13) Jazwinski, A.H.
Stochastic processes and filtering theory,
Ac. Press New York, London, 1970

(14) Kwakernaak, H., Sivan, R.
Linear optimal control systems,
Wiley Interscience, New York, 1972

(15) Lawson, C.L., Hanson, R.J.
Solving Least Squares Problems,
Prentice Hall, Englewood Cliffs, 1974

(16) Doekes, G., Simons, J.L.
Theoretical considerations on program PIAS (Processing of dynamic manoeuvre measurements with an Interactive Adaptive System). To be published.

(17) Doekes, G., Simons, J.L.
Users manual of program PIAS (Processing of dynamic manoeuvre measurements with an Interactive Adaptive System),
NLR Memorandum WN-78-005, 1978

(18) Doekes, G., Simons, J.L.
Description of program PIAS (Processing of dynamic manoeuvre measurements with an Interactive Adaptive System),
NLR Memorandum WN-78-006, 1978